Electronic Supplementary Material (ESI) for ChemComm.

Electronic Supplementary Information

Reversible Photo-patterning of Soft Conductive Materials *via* Spatially-defined Supramolecular Assembly

Xun He, Jingwei Fan, Jiong Zou, Karen L. Wooley*

Departments of Chemistry, Chemical Engineering, and Materials Science and Engineering, Laboratory for Synthetic-Biologic Interactions
Texas A&M University, P.O. BOX 30012, 3255 TAMU
College Station, TX 77842 (USA)
** Corresponding author email: wooley@chem.tamu.edu*

Table of Contents

Materials. Ethyl acetate, *n*-hexane, tetrahydrofuran (THF), diethyl ether, *N,N*-dimethylformamide (DMF, anhydrous, ≥ 99.8%), trifluoroacetic acid (TFA), *α*-pinene, triphosgene, and single-walled carbon nanotube (SWCNT, product number 724777, prepared by CoMoCAT® Catalytic Chemical Vapor Deposition (CVD) Method, 90% carbon and 10% non-carbon composition, ≥80.0% carbon as SWCNT, diameter 0.7-1.4 nm, median length 1.10 μm) were purchased from Sigma-Aldrich Company (USA). DL-Allylglycine was received from Chem-Impex International, Inc. (USA). α-Methoxy-ω-amino polyethylene glycol (product number: 122000-2, M_n = 2000 g/mol) was purchased from Rapp Polymere (Germany). All chemicals were used without further purification, unless otherwise noted. Nanopure water (18 MΩ·cm) was acquired by means of a Milli-Q water filtration system, Millipore Corp (USA).

Characterization Techniques. ^{1}H and ^{13}C NMR spectra were recorded on a Varian Inova 500 spectrometer interfaced to a UNIX computer using VnmrJ software. Chemical shifts were referenced to the solvent resonance signals. Attenuated total reflection Fourier transform infrared spectroscopy (ATR-FTIR) spectra were recorded on an IR Prestige 21 system (Shimadzu Corp.) and analyzed using IRsolution v. 1.40 software. Ultraviolet visible spectroscopy (UV/Vis) absorption measurements were made using a UV-2550 system (Shimadzu Corp.). Measurements were performed in nanopure water in cuvettes with path lengths of 1 cm. Thermogravimetric analysis (TGA) was performed under argon atmosphere using a Mettler Toledo model TGA/DSC 1 (Mettler Toledo), with a heating rate of 10 °C/min. Measurements were analyzed using Mettler Toledo STAR^e v. 7.01 software. Glass transition temperatures (T_g) were measured by differential scanning calorimetry (DSC) on a Mettler Toledo DSC822®, with a heating rate of 5 °C/min and a cooling rate of 5 °C/min. Measurements were analyzed using Mettler Toledo STAR^e v. 7.01 software. The T_g was taken as the midpoint of the inflection tangent, upon the third heating scan. Dynamic mechanical analysis (DMA) was performed on a Mettler Toledo TT-DMA system. DMA measurements of the hydrogels were performed through compression on a 3.3 mm thick, 10 mm diameter cylinder. Dynamic measurements were recorded over a range of 0.1 to 10 Hz at room temperature with 5% compression and a dynamic force applied to provide ± 5% deformation. Kinetic data presented were obtained as a single exponential decay using Origin Pro 8.1 software. Transmission electron microscopy (TEM) images were collected on a JEOL 1200 EX operating at 100 kV and micrographs were recorded at calibrated magnifications using a SLA-15C CCD camera. Samples for TEM measurements were prepared as follows: 10 μL of the dilute solution was deposited onto a carbon-coated copper grid, and after 2 min, the excess of the solution was quickly wicked away by a piece of filter paper. Some of the indicated samples were then negatively stained with 1 wt% phosphotungstic acid (PTA) aqueous solution. After 30 s, the excess staining solution was quickly wicked away by a piece of filter paper and the samples were left to dry under vacuum overnight. The widths of the nanotubes were obtained by counting multiple (> 5) tubes at 100 positions in the TEM images, an average value with standard deviation for a sample was calculated accordingly. Scanning electron microscopy (SEM) imaging was performed in JOEL JSM-6400 SEM operated at an acceleration voltage of 15 kV. The preparation of samples for SEM involved placing a drop of hydrogel on a carbon thin film. The gel was then subjected to immediate freezing by liquid nitrogen, followed by lyophilization for 3 days. The surface of the resulting aerogel was sputter coated with gold for 3 min under argon before imaging. Sonication was performed in an ultrasonic homogenizer (maximum power, 150 W, 20 kHz, Model 150 V/T, Biologics, Inc.) equipped with a micro tip with a diameter of 3.81 mm, employing the power output of 30 W in the frequency of 20 kHz at room temperature. Photo-triggered sol-to-gel transition was performed through irradiation from a 532 nm continuous wave diode-pumped solid-state laser (250 mW). Heat-pressing was performed using a hydraulic hot-press 3912 system (Carver, Inc.), composite films were compressed with a force of 4.5 metric tons under 80 °C for 10 min. Four-point probe measurements were done with an Agilent Digital Multimeter (Agilent Technology) with the tip spacing set at 1.6 mm. The average electrical conductivity values were obtained by measuring four different locations on the same film sample after hot-press. Conductivities were calculated according to $\sigma = I \cdot C^{-1} V^{-1} t^{-1}$, where V and I were obtained from the digital multimeter, C is a correction factor related the film diameter[1], and t is the film thickness measured by a micrometer at multiple positions (> 5) of a film.

Synthesis of DLAG-NCA monomer. DL-Allylglycine (10.0151 g, 86.99 mmol) and triphosgene (14.5318 g, 48.97 mmol) were stirred in a mixed solvent of dry THF (300 mL) and α-pinene (34 mL) for 2.5 h at 50 °C under N_2. The solution was concentrated, then precipitated twice into hexane, recrystallized twice from ethyl acetate/hexane, and dried under vacuum; which gave a white needle-like solid in a yield of 4.744 g (38.6%). ^{1}H NMR (500 MHz, $CDCl_3$-d, δ): 2.53 and 2.72 (m, 2 H, CH_2), 4.40 (m, 1 H, C*H*), 5.28 (m, 2 H, H_2C=CH), 5.75 (m, 1 H, H_2C=C*H*), 6.52 (br, 1 H, N*H*). ^{13}C NMR (125 MHz, $CDCl_3$-d, δ): 36.0 (CH*C*H_2CH), 57.3 (NH*C*H(CO)CH_2), 121.61 (CH=*C*H2), 130.0 (CH_2*C*H=CH_2), 152.5 (NH*C*OO), 168.9 (O*C*OCH). FT-IR: *v* = 3345 (s), 3095 (w), 3017 (w), 2934 (w), 1842 (m), 1827 (s), 1748 (vs), 1290 (s), 926 (vs) cm^{-1}. HRMS (ESI, m/z): $[M - H]^-$ calcd for $C_6H_7NO_3$: 140.0348, found: 140.0345.

Synthesis of PEG-*b*-PDLAG diblock copolymer. A typical procedure for the preparation of PEG-*b*-PDLAG was as follows: into a flame-dried 250 mL Schlenk flask equipped with a stir bar and capped with a rubber septum with a needle outlet connected to a tube filled with drying agent, DLAG-NCA (2.6160 g, 18.54 mmol) in DMF (150 mL) was injected. After being stirred at room temperature for 5 min, $mPEG_{45}$-NH_2 (1.2317 g, 615.9 μmol) in DMF (10 mL) was injected *via* a syringe. The reaction mixture was stirred at room temperature (stir rate = 800 rpm) under continuous nitrogen flow (flow rate = 100 mL min^{-1}) for 48 h. The reaction mixture was then precipitated into diethyl ether (1 L) three times. The diblock copolymer was centrifuged, collected, and dried *in vacuo* to yield 2.1480 g (71.2%) as a white powder. ^{1}H NMR (500 MHz, TFA-d, δ): 2.65 (br, 60 H, CHCH_2CHCH_2), 3.63 (s, 3 H, CH_3O), 3.97 (br, 180 H, OC$H_2$$CH_2$), 4.78 (br, 30 H, NHC*H*CO), 5.27 (br, 60 H, CH_2CHCH_2), 5.76 (br, 30 H, CH_2C*H*CH_2). ^{13}C NMR (125 MHz, TFA-d, δ): 38.5 (CH*C*H_2CH), 56.1 (NH*C*H(CO)CH_2), 59.9 (*C*H_3O), 71.9 (CH_2*C*H_2O), 122.2 (CH=*C*H2), 132.6 (CH_2*C*H=CH_2), 175.7 (NH*C*(CO)CH_2). FT-IR: v = 3426-3149 (m), 3079 (w), 2871 (m), 1697 (m), 1627 (vs), 1515 (s), 1103 (vs), 701 (m) cm^{-1}. DSC: T_g = -63 °C, T_c = -40 °C, T_m = 10 °C, T_g = 78 °C. TGA: 25-340 °C: 0% mass loss, 340-430 °C: 73.3% mass loss, 430-500 °C: 1.4% mass loss, 25.3% mass remaining above 500 °C.

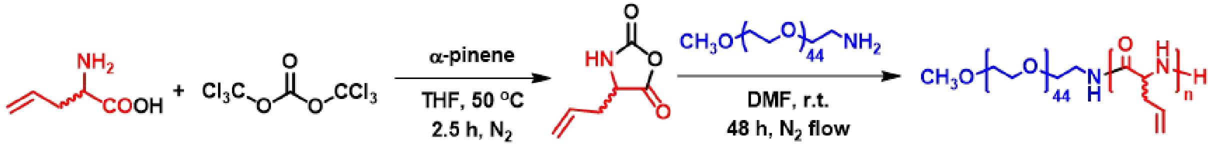

DLAG-NCA

PEG-*b*-PDLAG

Figure S1. Synthetic route for PEG-*b*-PDLAG block copolymer.

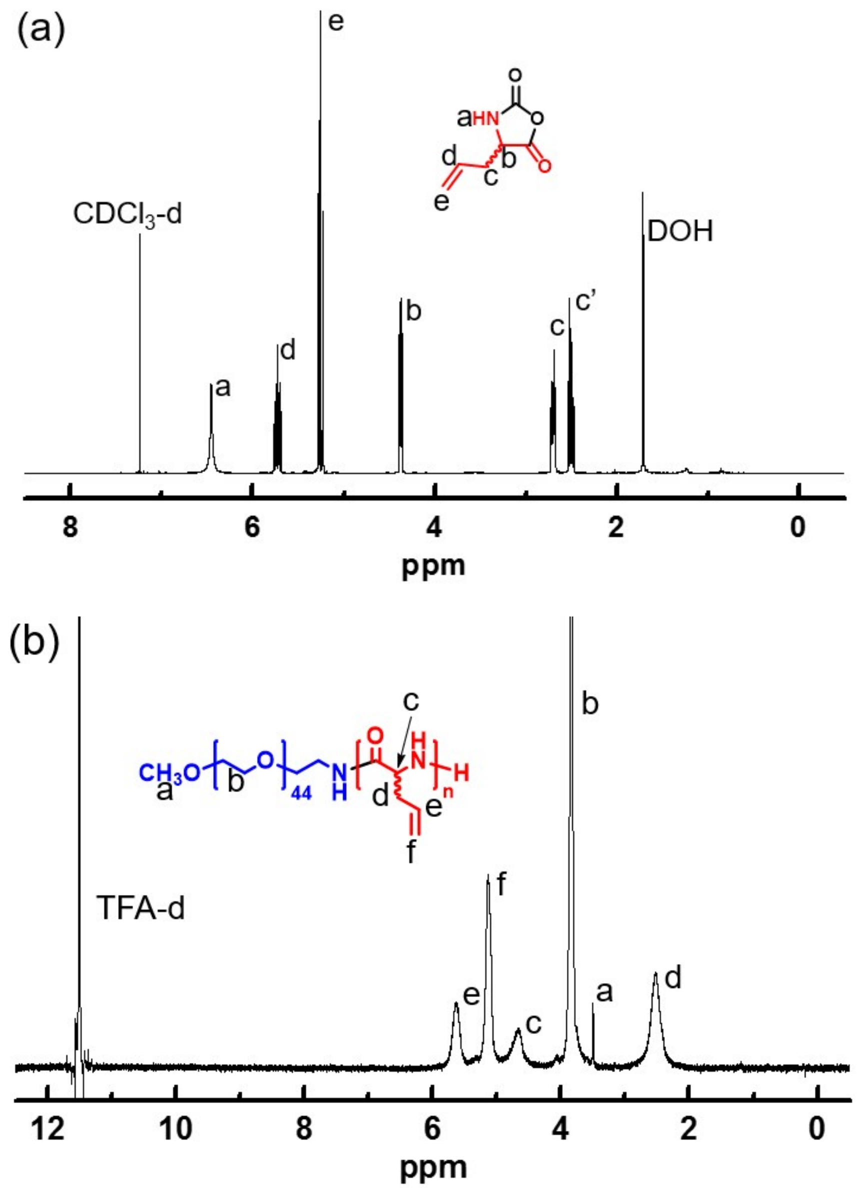

Figure S2. ^{1}H NMR of (a) DLAG-NCA monomer and (b) PEG-*b*-PDLAG block copolymer.

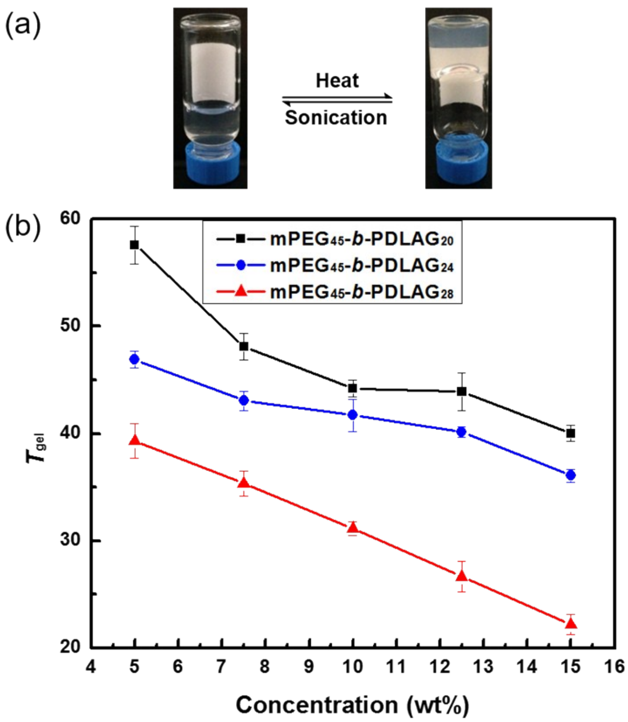

Figure S3. (a) Stimuli-responsive reversible sol-gel transitions of PEG-*b*-PDLAG block copolymer in water. (b) Change of T_{gel} as a function of polymer concentration for a series of PEG-*b*-PDLAG, having consistent PEG chain length and variation of the PDLAG chain lengths.

Hydrogelation of PEG-b-PDLAG. Hydrogels were prepared by direct dissolution of PEG-b-PDLAG in water, followed by heating above the sol-to-gel transition temperature (T_{gel}), which was determined by the test tube inversion method. In order to improve the stimuli-responsive sensitivity and achieve rapid response for printing and injection applications, we optimized the T_{gel} of the diblock gelator through control of the hydrophilic-hydrophobic balance, which could be tuned by the number of repeating units of the polypeptide block segment. According to Figure S3b, a lower T_{gel} transition temperature can be achieved through extension of the PDLAG block, which strengthens the physical interactions between polymer chains and facilitates the supramolecular assembly process.

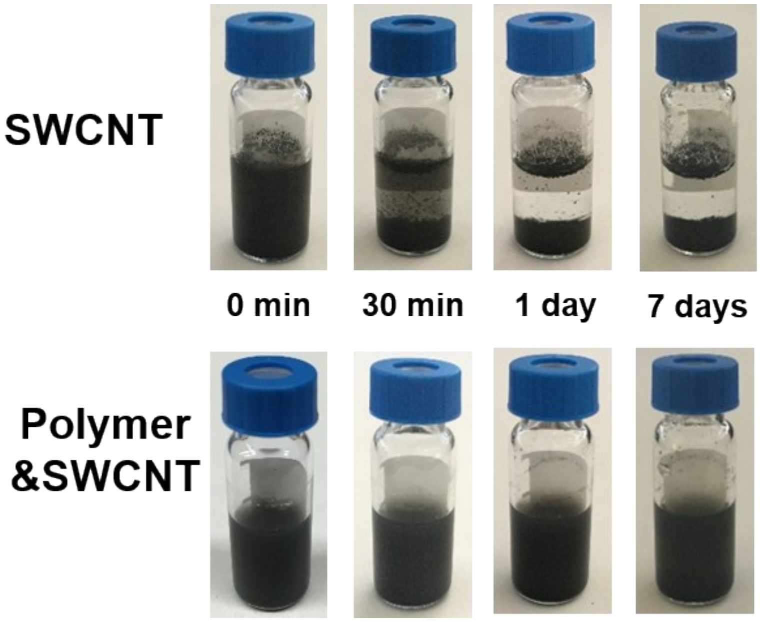

Figure S4. Images of SWCNTs in H_2O without (upper images) and with polymer (lower images), correlated with various time points after sonication (1 mg/mL SWCNTs, 0 or 10 mg/mL polymer).

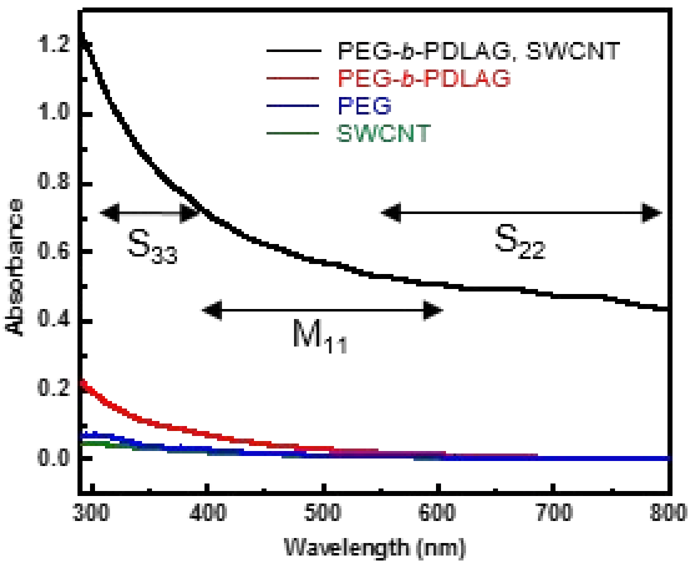

Figure S5. UV/vis spectra of assorted systems (with 0.05 mg/mL SWCNTs, 1 mg/mL polymer, if applicable).

The UV/vis absorbance spectra illustrate comparatively high absorbance through the entire measured range for the PEG-*b*-PDLAG/SWCNT composite, while SWCNT in water barely displayed any absorbance due to precipitation.

S_{33} refers to third order Van Hove singularities of semiconducting SWCNTs, M_{11} refers to first order Van Hove singularities of metallic SWCNTs, and S_{33} refers to second order Van Hove singularities of semiconducting SWCNTs.[2, 3]

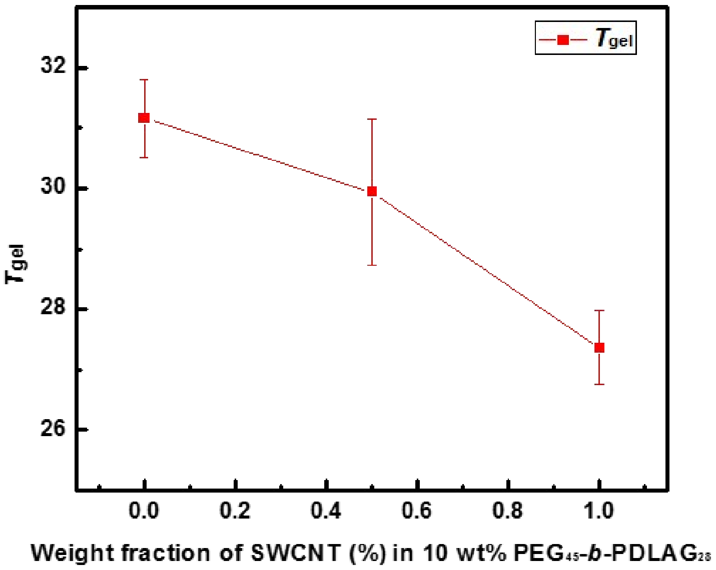

Figure S6. Incorporation of SWCNTs increased the thermal responsive sensitivity of the composite gel materials.

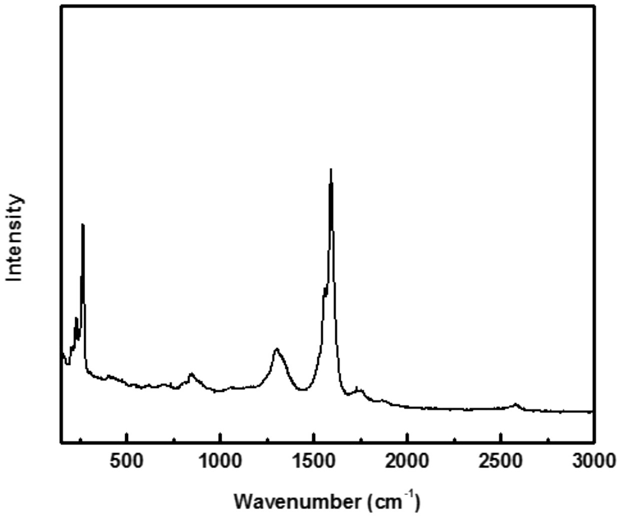

Figure S7. Raman spectrum of SWCNTs in solid form.

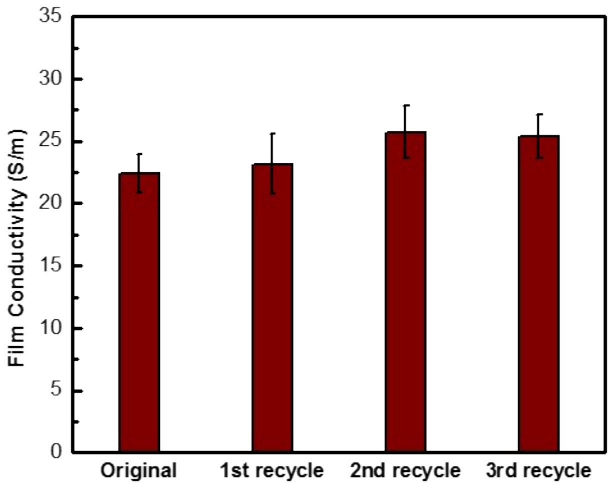

Figure S8. Conductivities of films composed of 15 wt% of SWCNTs and 85 wt% of PEG_{45}-*b*-$PDLAG_{28}$. One recycle process involves resuspension of the composite into water with sonication, responsive sol-to-gel transition, and film formation through air drying.

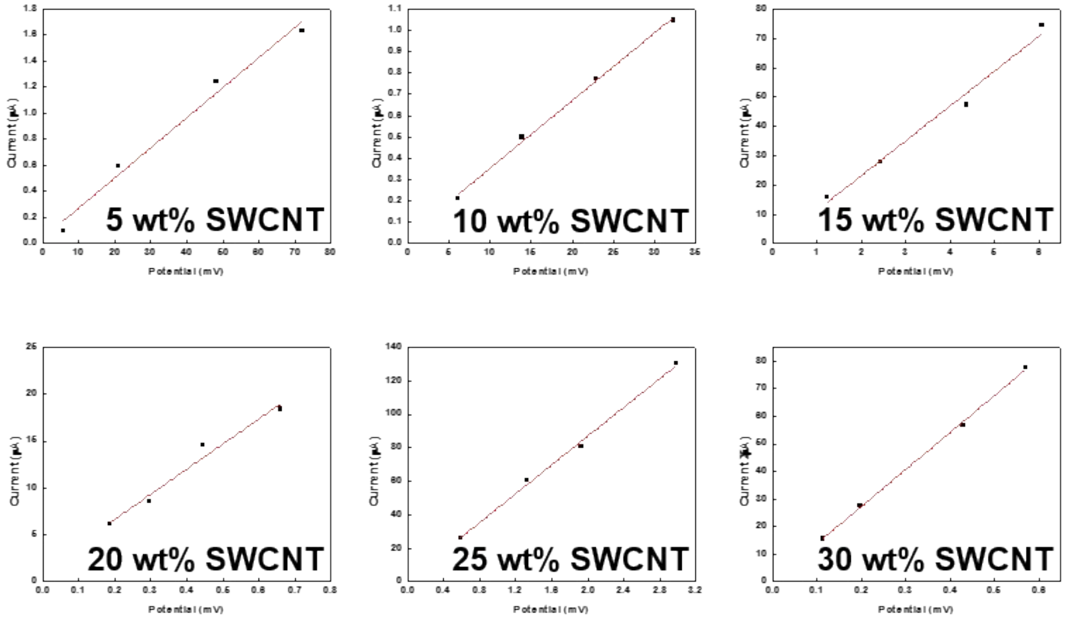

Figure S9. Linear fitted I-V curves of composite films with various percentage of SWCNT incorporation. Each spot was generated by measuring conductivity at a different location.

Table 1. Sheet resistance, thickness, and electrical conductivity of composite films as a function of percentage of SWCNT incorporation.

Loading of SWCNT (wt%)	Sheet resistance R_s (Ω/sq)	Film thickness t (μm)	Electrical conductivity σ (S/m)
5	$(2.1\pm0.8)\times10^{5}$	79±1	$(6.0\pm2.2)\times10^{-2}$
10	$(1.1\pm0.2)\times10^{5}$	77±6	$(1.2\pm0.2)\times10^{-1}$
15	$(4.0\pm0.3)\times10^{2}$	112±1	$(2.2\pm0.2)\times10^{1}$
20	$(1.2\pm0.2)\times10^{2}$	102±1	$(8.0\pm1.0)\times10^{1}$
25	$(9.0\pm0.4)\times10^{1}$	85±1	$(1.3\pm0.1)\times10^{2}$
30	$(2.9\pm0.1)\times10^{1}$	119±22	$(2.9\pm0.6)\times10^{2}$

1. F. M. Smits, *Bell Syst. Tech. J.*, 1958, **37**, 711-718.
2. H. Liu, D. Nishide, T. Tanaka and H. Kataura, *Nat. Commun.*, 2011, **2**, Article number: 309.
3. C. Backes, F. Hauke and A. Hirsch, *Adv. Mater.*, 2011, **23**, 2588-2601.